European Neolithic societies showed early warning signals of population collapse

Sean S. Downey[a,1], **W. Randall Haas Jr.**[a], **and Stephen J. Shennan**[b]

[a]Anthropology Department, University of Maryland, 4302 Chapel Lane, College Park, MD 20742; and [b]Institute of Archaeology, University College London, London WC1H 0PY, United Kingdom

Edited by Timothy A. Kohler, Washington State University, Pullman, WA, and accepted by Editorial Board Member James O'Connell June 30, 2016 (received for review March 16, 2016)

Ecosystems on the verge of major reorganization—regime shift—may exhibit declining resilience, which can be detected using a collection of generic statistical tests known as early warning signals (EWSs). This study explores whether EWSs anticipated human population collapse during the European Neolithic. It analyzes recent reconstructions of European Neolithic (8–4 kya) population trends that reveal regime shifts from a period of rapid growth following the introduction of agriculture to a period of instability and collapse. We find statistical support for EWSs in advance of population collapse. Seven of nine regional datasets exhibit increasing autocorrelation and variance leading up to collapse, suggesting that these societies began to recover from perturbation more slowly as resilience declined. We derive EWS statistics from a prehistoric population proxy based on summed archaeological radiocarbon date probability densities. We use simulation to validate our methods and show that sampling biases, atmospheric effects, radiocarbon calibration error, and taphonomic processes are unlikely to explain the observed EWS patterns. The implications of these results for understanding the dynamics of Neolithic ecosystems are discussed, and we present a general framework for analyzing societal regime shifts using EWS at large spatial and temporal scales. We suggest that our findings are consistent with an adaptive cycling model that highlights both the vulnerability and resilience of early European populations. We close by discussing the implications of the detection of EWS in human systems for archaeology and sustainability science.

archaeology | early warning signs | human paleodemography | Neolithic Europe | resilience

A 2012 Special Issue in PNAS debates how analysis of historical collapse in ancient societies can contribute to sustainability science (1). Key themes include accounting for complexity and multicausality in instances of collapse, modeling, and predicting both short- and long-term environmental change and the importance of historical and archaeological case studies. Although significant progress has been made in measuring ecosystem resilience and predicting collapse (2), quantifying the resilience of human societies presents a major challenge for social science research (3, 4). Further, the use of archaeological data and EWS methods to predict known periods of collapse in ancient human societies (i.e., retrodiction) (5) remains largely unexplored. Resilience as we use the concept here is defined as the ability of a system to absorb change and recover from disturbance while maintaining relationships between populations or state variables (6). Recent developments in ecology point to a promising new direction that follows from the observation that ecosystem resilience tends to decrease in advance of regime shifts—major transitions among qualitatively distinct ecosystem states (7). Theoretical and empirical studies of nonhuman systems reveal that decreasing resilience is detectable via time series statistics termed early warning signals (EWSs) (8). Although regime shifts are well documented in human-dominated ecosystems (9–13), the degree to which EWSs anticipate them remains largely unexamined due to data limitations at requisite spatial and temporal scales. However, recent advances in the integration of large-scale archaeological data (14–16) are narrowing the gap between theory and data. This study presents what we believe to be the first statistical evidence for EWSs of regime shifts in human population dynamics.

Our case studies include 2,378 archaeological sites from nine regions of Neolithic Europe, ca. 8–4 kya. Previous research has observed evidence of major demographic regime shifts in the form of large-scale boom-bust dynamics among many of these Neolithic cases (17). Estimated population declines range from 20% to 60% in as little as a century. The population proxies that revealed these boom-bust dynamics are based on the temporal frequencies of radiocarbon-dated archaeological sites, which are represented as summed probability densities (SPDs). This site-based population proxy assumes that the temporal frequencies of occupied human settlements in a given region index relative human population size. Use of SPD-based approaches to inferring population change has been debated in the literature (18–26). Critics have raised concerns about confounding factors including atmospheric effects, sampling biases, taphonomic processes, or calibration error; however, the methods used here and elsewhere (20) attempt to control for these sources of error by (*i*) correcting systematic biases in the data and (*ii*) comparing the corrected empirical patterns to null SPD models that simulate exogenous processes. Thus, current SPD methods reflect a significantly more conservative version of the approach that Rick (27) originally proposed.

We analyze archaeological SPDs for two classes of EWSs: critical slowing down (CSD) and flickering. CSD describes a general increase in the time it takes a system to recover from external

Significance

This study explores whether archaeologically detectable declines in resilience precede the onset of large-scale human population collapses. Our case study is the European Neolithic: a period that began approximately 9,000 y ago when the introduction of agricultural technologies initiated phases of rapid population growth that were in many cases followed by demographic instability and dramatic collapse. Our study finds evidence that statistical signatures of decreasing resilience can be detected long before population decline begins. To our knowledge, this study is the first to find early warning signals of demographic regime shift among human populations. The results suggest that archaeological information can potentially be used to monitor social and ecological vulnerability in human societies at large spatial and temporal scales.

Author contributions: S.S.D. designed research; S.S.D., W.R.H., and S.J.S. performed research; S.S.D. and W.R.H. contributed new reagents/analytic tools; S.S.D. and W.R.H. analyzed data; and S.S.D., W.R.H., and S.J.S. wrote the paper.

The authors declare no conflict of interest.

This article is a PNAS Direct Submission. T.A.K. is a Guest Editor invited by the Editorial Board.

Freely available online through the PNAS open access option.

[1]To whom correspondence should be addressed. Email: sdowney2@umd.edu.

This article contains supporting information online at www.pnas.org/lookup/suppl/doi:10.1073/pnas.1602504113/-/DCSupplemental.

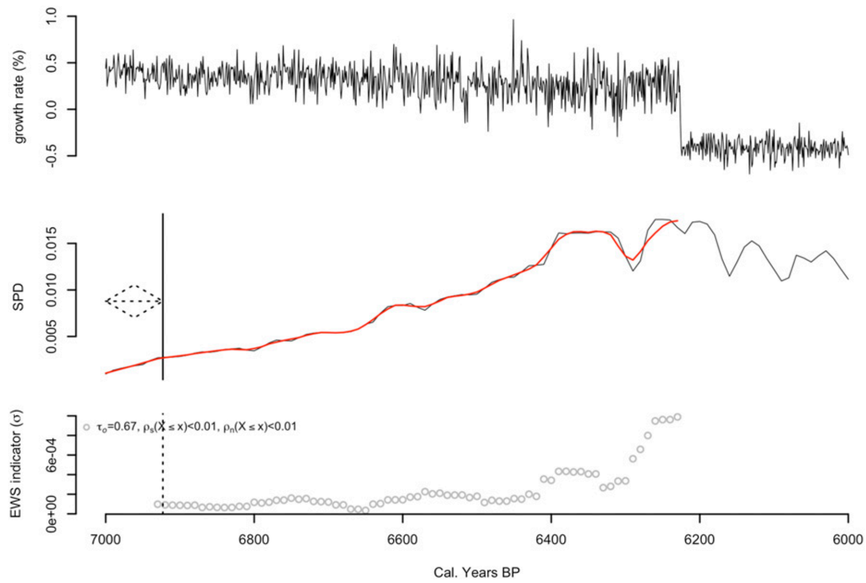

Fig. 1. A regime shift model of population growth rate variability, radiocarbon date calibration, and EWSs that demonstrates CSD in growth rates can be recovered from simulated SPDs.

shocks such as population loss due to disease, warfare, or crop failure. Flickering describes increasing directional bias in a system's response rate to such perturbations, such as a society stuck in a socio-ecological trap where strong reinforcing behavior and a lack of innovation prevents adaptation (28–30). Here, flickering would suggest increasing recovery time from population decline events relative to growth events before major collapse. Because a number of nonhuman biological populations exhibit critical slowing down and flickering in advance of regime shifts (31–38), we consider the possibility that these EWS indicators could also be detected in long-term human population dynamics as viewed through archaeological proxies.

Results

CSD Detection with a Simulated Demographic Regime Shift and an Archaeological Deposition Process Model. Fig. 1 illustrates how CSD can be detected in a model system that transitions from a high growth regime to low growth. In the model, slowly decreasing human population growth rates and increasing variance precedes the transition to the low growth regime. These simulated growth rates are used to simulate an archaeological SPD including deposition processes, taphonomic decay, atmospheric effects, radiocarbon calibration, and isotopic counting error processes (*Materials and Methods*). The SPD is then evaluated for EWSs using the same statistical procedures we use in the empirical analysis. Declining resilience is indicated in the bottom panel by the increasing EWS indicator values up to the point of collapse. The EWS indicator increase is statistically significant using the individual tau observations (τ_s) and with a robust statistical test (τ_n). Empirically, any of a number of drivers such as changing climate, declining environmental productivity, disease, warfare, or some combination thereof could produce these results.

Results for All European Neolithic Regions. Qualitative EWS trends are evident in many cases (Table S1 and Dataset S1), leading us to perform quantitative tests (see Fig. S1 and *SI Text*, *Early Warning Signals of Collapse in Neolithic Paris Basin* for an illustrative example). Table 1 presents the results of $\tau_{[o]}$ for the three EWS metrics, including their associated statistical strengths ($P_{[s]}$). All but 2 of the 27 tests produced statistically significant results ($P_{[s]} < 0.1$), indicating that statistical effects are unlikely to account for the observed EWSs. However, these standard probability tests for $\tau_{[o]}$ do not distinguish between EWSs produced by Neolithic demographic processes and those produced by the confounding factors, so we next compare the empirical tau values to a simulated null model. This comparison shows that in

Table 1. EWS analysis results of summed probability distributions of nine European regions

	AR (1)			σ			1γ		
Region	$\tau_{[o]}$	$P_{[s]}$	$P_{[n]}$	$\tau_{[o]}$	$P_{[s]}$	$P_{[n]}$	$\tau_{[o]}$	$P_{[s]}$	$P_{[n]}$
Southern Germany	0.54	0.00***	0.04**	0.89	0.00***	0.32	−0.78	0.00***	0.04**
Eastern Switzerland	0.59	0.00***	0.05**	0.13	0.11	0.47	−0.47	0.00***	0.14
England and Wales (without Wessex and Sussex)	0.49	0.00***	0.04**	0.96	0.00***	0.01***	−0.51	0.00***	0.14
Ireland	0.70	0.00***	0.01***	0.96	0.00***	0.03**	−0.37	0.00***	0.27
Paris Basin	0.65	0.00***	0.01***	0.97	0.00***	0.09*	−0.30	0.00***	0.18
Rhone-Languedoc	0.65	0.00***	0.09*	0.95	0.00***	0.04**	−0.79	0.00***	0.27
Scotland	0.49	0.00***	0.03**	0.95	0.00***	0.02**	−0.09	0.31	0.42
Southern England (Wessex and Sussex)	0.42	0.04**	0.17	0.68	0.00***	0.06*	−0.44	0.00***	0.13
Western France	0.48	0.02**	0.14	0.62	0.00***	0.04**	−0.36	0.02**	0.37

Significance levels: $*P = 0.10$; $**P = 0.05$; $***P = 0.01$.

Table 2. **Fisher's exact tests for multiple analyses**

Tau ($\tau_{[o]}$)	EWS	Pass†	Fail†	CI low	CI high	P‡
Sample ($P_{[s]}$)	AR (1)	9	0	6.67	Infinity	0.00***
	σ	8	1	3.54	4,053.00	0.00***
	1γ	8	1	3.54	4,053.00	0.00***
Null model ($P_{[n]}$)	AR (1)	7	2	2.20	1,854.15	0.00***
	σ	7	2	2.20	1,854.15	0.00***
	1γ	1	8	0.02	117.49	1.00

Significance level: ***P = 0.01. CI, confidence interval.

†Pass/fail at P < 0.1.

‡Expected ratio used in Fisher test is 1:8, pass:fail.

seven of nine regions, both AR (1) and σ exhibit increases that are significantly different from those produced by the null model ($P_{[n]} < 0.1$). Conversely, 1γ produces only one result of nine that is significantly different from the tau values produced by the null model. We conclude that confounding factors (*i*) are unlikely to account for the majority of CSD patterns in the empirical data but (*ii*) can account for the majority of skewness patterns in the data.

Table 2 considers whether the multiple statistically significant results could be obtained by chance given $P_{[n]}$ values that are uniformly distributed between 0 and 1. For each set of nine $P_{[n]}$ outcomes for AR (1), σ, and 1γ, Fisher's exact tests for AR (1) (7:2) and σ (7:2) show that the empirical results are unlikely to be explained by sampling effects ($P < 0.01$), whereas 1γ (1:8) can be explained by sampling effects ($P = 1$). In sum, the data from all regions reveal evidence of CSD but flickering does not appear to be a useful indicator of population collapse.

Discussion

It is unsurprising that societies on the verge of collapse may exhibit warnings signs; yet it is difficult to demonstrate such phenomena empirically. Our results support the hypothesis that CSD was present in Neolithic Europe demographics, detectable in archaeological SPD curves, and that the EWSs are not artifacts of sampling or confounding effects. This surprising finding encourages us to explore systemic relationships between human paleodemography and CSD and to consider the implications for human ecosystem monitoring (see also *SI Text*, *Theoretical Considerations Related to SPD-Based EWSs Among Human Societies*).

Regime Shifts in Human Societies. Human population dynamics are known to exhibit multidimensional and nonlinear processes; therefore, regime shifts and EWSs should also be expected. Equilibrium, multiple stable population points, and chaotic regimes are all known to emerge from even the simplest demographic models (39). When density-dependent population feedbacks, or Allee affects, interact with logistic growth and environmental perturbations, critical transitions may ensue (6, 40). Allee effects and logistic growth processes have been observed or suspected in many biological populations including yeast, plants, shellfish, and humans (41–43). Moreover, human systems involve cross-generational effects of past environments on the population levels of later generations (44, 45). For example, dramatic environmental change, warfare, disease, or complex interactions among these mechanisms may lead to population collapse. Regime shifts and CSD should therefore be expected in at least some human population dynamics.

A Framework for Interpreting EWSs Among Human Populations at Large Spatial and Temporal Scales. Following a recent theoretical synthesis on resilience in socio-ecological systems (46), we consider the following three generic mechanisms that may offer insights into the general mechanisms of regime shifts in human systems over large spatial and temporal scales: (MI) a slowly changing driver to tipping point, (MII) interaction of fast and slow cycles, and (MIII) large but infrequent changes in external drivers.

MI entails an external driver that slowly forces a system across a tipping point to a qualitatively different state. Such critical transitions entail feedback loops that create the context for nonlinear responses to linear changes in the external driver (37). As noted above, Allee effects can trigger critical transitions, and several authors (37, 47) propose that Neolithic population collapse in the US Southwest and among human societies more generally can be understood as critical transitions [see also (48)]. As resource availability steadily declines, sunk-cost effects can generate adaptive feedback loops that artificially lock humans into maladaptive strategies such as remaining in established settlements until the exogenous driver eventually forces the system across a tipping point into an alternative adaptive regime. Continuing on such unsustainable courses in the face of steady resource decline ultimately leads to catastrophic failure. More recently, Lade et al. (49) show that common-pool resource management systems can create a context for critical transitions in human societies when external drivers slowly force systems to alternative states.

In MI systems, the timing of regime shifts can be predicted at the point when variance and autocorrelation reach infinity, known technically as a bifurcation point (or tipping point). However, reaching a bifurcation point would only happen under stringent conditions, and stochasticity in real-world systems will tend to trigger regime shifts before the theoretical transition; for example, in early agricultural societies (Fig. S2). Regardless, CSD should precede the regime shift (46). Of the three mechanisms discussed here, only MI causes true critical transitions with bifurcations. As a result, reducing or reversing the driver variable after a bifurcation will not return the system to the previous regime without resetting other system parameters (i.e., hysteresis). The other two mechanisms also cause regime shifts, but because recovery is possible and the changes are not permanent, these are not considered critical transitions (46).

MII describes interaction between slow and fast cycles that can cause dramatic regime shifts without bifurcation. For example, annual cultivation cycles in agricultural systems that involve forest clearing (i.e., swidden or slash-and-burn) are highly constrained by soil fertility and biomass recovery dynamics occurring over decades. Repeated and intensive forest cultivation can cause local resources to become depleted and ultimately trigger the abandonment of settlements, but eventually forests and soils can recover and abandoned settlements may be reoccupied. Many types of environmental and human cycling exist that could lead to interactions and regime shifts, including environmental overexploitation and recovery (45, 50), biogeochemical cycling (51), land surface change (2), climate cycling (52), epidemiology (53), human demography (13), and episodes of human violence (54, 55). These dynamics are predicted to exhibit the statistical signatures of CSD (46).

In MIII systems, a large but infrequent change in external conditions forces a system into another state. For example, catastrophic population losses could result from unusual natural disasters (56, 57), the emergence of genetically novel disease transmission vectors [e.g., airborne transmission of *Yersinia pestis* (58) and the Black Death (59)], social conflict at novel scales of severity (e.g., World War I), or extreme and rare climatic events such as volcanic eruptions (e.g., Pompeii). However, the demographic system itself is not trapped at low levels and may eventually recover. EWSs are not expected in such cases (46).

Implications for Understanding the Causes of Collapse During the European Neolithic. The EWS analysis of Neolithic Europe population dynamics tends to exhibit EWSs in AR (1) and σ, suggesting that MI and MII are plausible and that MIII is unsupported. However, determining which of the two potential regime shift mechanisms is the more plausible explanation for a pattern of collapse occurring independently at different times and in different regions throughout Europe cannot be determined from the EWS

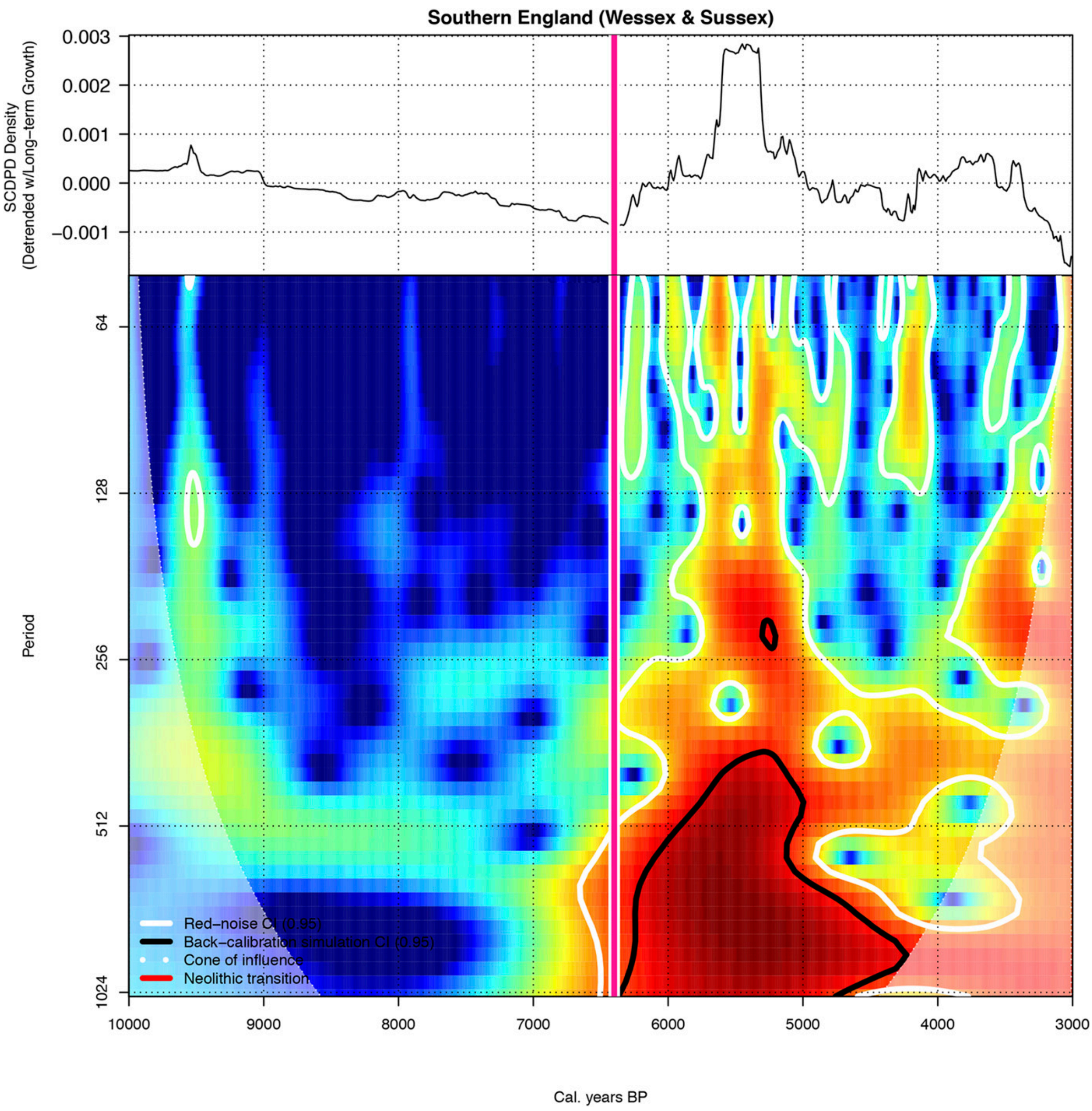

Fig. 2. Wavelet analysis of Southern England showing Neolithic transition date (red line), periods of significant cycling and frequency using a Gaussian noise (white highlight), and the SPD null model (black highlight).

analysis alone. Instead, we use wavelet analysis to test the expectation of an MII slow-fast cycling mechanism (*SI Materials and Methods*). For example, the Wessex-Sussex region of England exhibits statistically significant cycling patterns in the SPDs (Fig. 2). In this case, the standard Gaussian white-noise filter identifies significant cycles at high frequencies that are probably associated with the radiocarbon date calibration process. However, when we use a noise filter based on the SPD null model distribution, the main statistically significant cycles remaining are around 5.5 kya with a frequency of between 400 and 1,000 y. The pattern holds for each of the nine regions (Dataset S1), and we find it to be in line with predictions from human demographic modeling (13). A possible explanation is that interactions between fast human demographic cycles and slower ecosystem recovery cycles may explain the observed pattern of demographic collapse in Neolithic Europe. Similar cycling patterns have been observed among prehistoric agrarian populations in the US Southwest (54, 55), and the hypothesis is consistent with recent paleoenvironmental research that finds correlations between deforestation and human population growth during the European Neolithic (60–62). Using the framework introduced in the previous section, this deforestation hypothesis would suggest that MII cycle interactions between rapidly increasing human population levels and environmental dynamics during the early Neolithic may have contributed to the observed demographic collapses.

Importantly, fast–slow cycle interactions in human societies are more consistent with adaptive cycles (3, 45) than Lotka–Volterra interactions. In contrast to the latter, adaptive cycling emphasizes collapse and reorganization that may or may not reproduce previous ecological states. Instead, each collapse is generally followed by a level of recovery that sometimes exceeded precollapse levels and was often accompanied by distinct socioeconomic structure (e.g., Bronze Age systems). Recovery may be understood as the outcome of adaptive reorganization on fundamentally altered cultural and natural landscapes. Such reorganization is generally expected among human populations with cumulative culture. In some cases, endogenous expansion-growth dynamics may have temporarily increased societal resilience to changing rates of climate variability (e.g., during Linear Pottery Culture) (63). Therefore, on one hand, some societies tended to experience quantifiable loss of resilience that led to dramatic declines in population levels; on the other hand, other societies recovered to generate larger and presumably more resilient populations. Where recovery did not occur, other societies with new adaptations moved in, as ancient DNA studies are beginning to show (64). As such, our results highlight both the vulnerability and the resilience of early European societies.

Conclusion: Prospects and Contributions to Archaeology and Sustainability Science

During the Neolithic revolution new agricultural technologies initiated rapid demographic growth, followed by periods of devastating societal instability that we are only now beginning to understand. It remains unclear whether modern technological innovation can continue to outpace demand, and it is important for sustainability scientists to consider the possibility that generic mechanisms can contribute to demographic collapse in human societies, as well as to develop ways to detect declining resilience. Here we present evidence that early warning signals preceded large-scale population collapse in the European Neolithic Period. To encourage further study of human ecodynamics, we include a framework for interpreting societal regime shift at large spatial and temporal scales that links three generic mechanisms that are known for causing social and ecological regime shifts with social processes such as growth and collapse, climate change, resource degradation, disease, and warfare. We suggest that complex interactions among social and natural factors, and emergent patterns such as Allee and sunk-cost effects, may slow the recovery of human societies during periods of decreased resilience. Further, distinct statistical signatures of declining resilience due to these processes are detectable despite the complex depositional processes that confound archaeological proxy data. We suggest that the detection of EWSs in human settlement patterns is a general finding that points to a need for EWS analyses of other types of archaeological data and other historical datasets. We believe our framework can provide a way to analyze complex dynamics in human ecosystems, and perhaps ultimately to monitor and prevent catastrophic consequences of societal regime shifts.

Materials and Methods

Archaeological Radiocarbon Database. The complete dataset includes archaeological radiocarbon dates comprising 2,759 sites for Mesolithic and Neolithic Europe, ca. 10–3.5 kya (65). Nine regions were selected for the EWS analysis because they provide the clearest qualitative and quantitative shifts from high to low growth regimes (Table S2).

Statistical Methods and SPD Modeling. To minimize the effects of sampling bias, radiocarbon calibration effects (66) and taphonomic bias (21), we use the Bchron R package (67), IntCal13 (68), and Monte Carlo simulation to generate a corrected SPD curve (Fig. S3). The EWS analysis involves isolating subsets from each time series from the Neolithic transition to the point of collapse, detrending the resulting time series, and calculating three EWS statistics including autocorrelation, variance, and skewness following ref. 69. EWS patterns are assessed qualitatively (Table S1), and statistically using the Kendall's tau rank correlation test with both an optimized tau value (Table 1) and the complete time series (Table S3). The procedures for generating a null model follow ref. 17 and the rigorous statistical test for examining the effects of confounding archaeological factors on the EWS analysis involves computing cumulative density functions from the null model and calculating the probabilities of each observed EWS statistic using single-tailed tests. Fisher's exact tests are used to determine the probability of the significant EWS statistics τ_o and $\tau_{[o]}$ for the optimized time series (Table 2) and for the full time series (Table S4). A sensitivity analysis evaluates the effect of sliding window size and the length of the time series on the significance of the EWS statistics (70) (Dataset S1). These EWS methods (Fig. S4), the simulation shown in Fig. 1, and the wavelet analysis (71, 72) are described in further detail in the *SI Materials and Methods*. All analyses are performed using R (73). Code is available on request.

ACKNOWLEDGMENTS. This work was funded by the Anthropology Department, the College of Behavioral and Social Sciences at the University of Maryland, and European Research Council Advanced Grant 249390 (to S.J.S.).

1. Butzer KW, Endfield GH (2012) Critical perspectives on historical collapse. *Proc Natl Acad Sci USA* 109(10):3628–3631.
2. Streeter R, Dugmore AJ (2013) Anticipating land surface change. *Proc Natl Acad Sci USA* 110(15):5779–5784.
3. Allen CR, Angeler DG, Garmestani AS, Gunderson LH, Holling CS (2014) Panarchy: Theory and application. *Ecosystems (N Y)* 17(4):578–589.
4. Redman CL (2005) Resilience theory in archaeology. *Am Anthropol* 107(1):70–77.
5. Noble IR (1996) Global change and terrestrial ecosystems. *International Geosphere-Biosphere Programme Book Series*, eds Walker B, Steffan B, No. 2 (Cambridge Univ Press, Cambridge, UK) pp. 173–183.
6. Holling CS (1973) Resilience and stability of ecological systems. *Annu Rev Ecol Syst* 4: 1–23.
7. Scheffer M, Carpenter S, Foley JA, Folke C, Walker B (2001) Catastrophic shifts in ecosystems. *Nature* 413(6856):591–596.
8. Scheffer M, Carpenter SR, Dakos V, Nes Ev (2015) Generic indicators of ecological resilience: Inferring the chance of a critical transition. *Annu Rev Ecol Evol Syst* 46(1): 145–167.
9. Tainter JA (1988) *The Collapse of Complex Societies* (Cambridge Univ Press, New York).
10. Diamond JM (2005) *Collapse: How Societies Choose to Fail or Succeed* (Viking, New York).
11. May RM, Levin SA, Sugihara G (2008) Complex systems: Ecology for bankers. *Nature* 451(7181):893–895.
12. Bocquet-Appel J-P (2011) When the world's population took off: The springboard of the Neolithic Demographic Transition. *Science* 333(6042):560–561.
13. Turchin P (2009) Long-term population cycles in human societies. *Ann N Y Acad Sci* 1162:1–17.
14. Kintigh KW, et al. (2014) Grand challenges for archaeology. *Proc Natl Acad Sci USA* 111(3):879–880.
15. van der Leeuw S, et al. (2011) Toward an integrated history to guide the future. *Ecol Soc* 16(4):2.
16. Dearing JA, Braimoh AK, Reenberg A, Turner BL, van der Leeuw S (2010) Complex land systems: The need for long time perspectives to assess their future. *Ecol Soc* 15(4):21.
17. Shennan S, et al. (2013) Regional population collapse followed initial agriculture booms in mid-Holocene Europe. *Nat Commun* 4:2486.
18. Williams AN (2012) The use of summed radiocarbon probability distributions in archaeology: A review of methods. *J Archaeol Sci* 39(3):578–589.
19. Collard M, Edinborough K, Shennan S, Thomas MG (2010) Radiocarbon evidence indicates that migrants introduced farming to Britain. *J Archaeol Sci* 37(4):866–870.
20. Timpson A, et al. (2014) Reconstructing regional population fluctuations in the European Neolithic using radiocarbon dates: A new case-study using an improved method. *J Archaeol Sci* 52:549–557.
21. Surovell TA, Byrd Finley J, Smith GM, Brantingham PJ, Kelly R (2009) Correcting temporal frequency distributions for taphonomic bias. *J Archaeol Sci* 36(8):1715–1724.
22. Ballenger JAM, Mabry JB (2011) Temporal frequency distributions of alluvium in the American Southwest: Taphonomic, paleohydraulic, and demographic implications. *J Archaeol Sci* 38(6):1314–1325.
23. Torfing T (2015) Neolithic population and summed probability distribution of 14C-dates. *J Archaeol Sci* 63:193–198.
24. Timpson A, Manning K, Shennan S (2015) Inferential mistakes in population proxies: A response to Torfing's "Neolithic population and summed probability distribution of 14C-dates". *J Archaeol Sci* 63:199–202.
25. Zahid HJ, Robinson E, Kelly RL (2016) Agriculture, population growth, and statistical analysis of the radiocarbon record. *Proc Natl Acad Sci USA* 113(4):931–935.
26. Downey SS, Bocaege E, Kerig T, Edinborough K, Shennan S (2014) The neolithic demographic transition in Europe: Correlation with juvenility index supports interpretation of the summed calibrated radiocarbon date probability distribution (SCDPD) as a valid demographic proxy. *PLoS One* 9(8):e105730.

SUSTAINABILITY SCIENCE

ANTHROPOLOGY

27. Rick JW (1987) Dates as data: An examination of the Peruvian Preceramic radiocarbon record. *Am Antiq* 52(1):55–73.
28. Boonstra WJ, de Boer FW (2014) The historical dynamics of social-ecological traps. *Ambio* 43(3):260–274.
29. Carpenter SR, Brock WA (2008) Adaptive capacity and traps. *Ecol Soc* 13:40.
30. Tschakert P, Shaffer LJ (2014) *Social-Ecological Systems in Transition* (Springer, New York), pp 139–156.
31. Carstensen J, Telford RJ, Birks HJB (2013) Diatom flickering prior to regime shift. *Nature* 498(7455):E11–E12.
32. Dakos V, van Nes EH, Scheffer M (2013) Flickering as an early warning signal. *Theor Ecol* 6(3):309–317.
33. Wang R, et al. (2012) Flickering gives early warning signals of a critical transition to a eutrophic lake state. *Nature* 492(7429):419–422.
34. Bailey RM (2011) Spatial and temporal signatures of fragility and threshold proximity in modelled semi-arid vegetation. *Proc Biol Sci* 278(1708):1064–1071.
35. Drake JM, Griffen BD (2010) Early warning signals of extinction in deteriorating environments. *Nature* 467(7314):456–459.
36. Scheffer M, et al. (2009) Early-warning signals for critical transitions. *Nature* 461(7260):53–59.
37. Scheffer M (2009) *Critical Transitions in Nature and Society* (Princeton Univ Press, Princeton).
38. Hefley TJ, Tyre AJ, Blankenship EE (2013) Statistical indicators and state–space population models predict extinction in a population of bobwhite quail. *Theor Ecol* 6(3): 319–331.
39. May RM (1976) Simple mathematical models with very complicated dynamics. *Nature* 261(5560):459–467.
40. Dai L, Vorselen D, Korolev KS, Gore J (2012) Generic indicators for loss of resilience before a tipping point leading to population collapse. *Science* 336(6085):1175–1177.
41. Taylor CM, Hastings A (2005) Allee effects in biological invasions. *Ecol Lett* 8(8): 895–908.
42. Steele J (2010) Radiocarbon dates as data: Quantitative strategies for estimating colonization front speeds and event densities. *J Archaeol Sci* 37(8):2017–2030.
43. Steele J (2009) Human dispersals: Mathematical models and the archaeological record. *Hum Biol* 81(2-3):121–140.
44. Benton TG, Plaistow SJ, Coulson TN (2006) Complex population dynamics and complex causation: Devils, details and demography. *Proc Biol Sci* 273(1591):1173–1181.
45. Gunderson LH, Holling CS, eds (2002) *Panarchy: Understanding Transformations in Human and Natural Systems* (Island Press, Washington, DC).
46. Dakos, V, Carpenter, S. R, Nes, E. H. v, Scheffer M. (2015) Resilience indicators: prospects and limitations for early warnings of regime shifts. *Philos Trans R Soc Lond B Biol Sci* 370:20130263.
47. Janssen MA, Kohler TA, Scheffer M (2003) Sunk-cost effects and vulnerability to collapse in ancient societies. *Curr Anthropol* 44(5):722–728.
48. Hegmon M, et al. (2008) Social transformation and its human costs in the prehispanic U.S. Southwest. *Am Anthropol* 110(3):313–324.
49. Lade SJ, Tavoni A, Levin SA, Schlüter M (2013) Regime shifts in a social-ecological system. *Theor Ecol* 6(3):359–372.
50. Lee CT, Tuljapurkar S (2008) Population and prehistory I: Food-dependent population growth in constant environments. *Theor Popul Biol* 73(4):473–482.
51. Folke C, et al. (2004) Regime shifts, resilience, and biodiversity in ecosystem management. *Annu Rev Ecol Evol Syst* 35:557–581.
52. Chavez FP, Ryan J, Lluch-Cota SE, Niquen C M (2003) From anchovies to sardines and back: Multidecadal change in the Pacific Ocean. *Science* 299(5604):217–221.
53. Althouse BM, Hébert-Dufresne L (2014) Epidemic cycles driven by host behaviour. *J R Soc Interface* 11(99):11.
54. Turchin P, Korotayev A (2006) Population dynamics and internal warfare: A reconsideration. *Social Evol History* 5(2):112–147.
55. Kohler TA, Cole S, Ciupe S (2009) *Pattern and Process in Cultural Evolution*, ed Shennan S (Univ of California Press, Berkeley), pp 277–295.
56. Firestone RB, et al. (2007) Evidence for an extraterrestrial impact 12,900 years ago that contributed to the megafaunal extinctions and the Younger Dryas cooling. *Proc Natl Acad Sci USA* 104(41):16016–16021.
57. Kuijt I (2001) Reconsidering the cause of cultural collapse in the Lillooet area of British Columbia, Canada: A geoarchaeological perspective. *Am Antiq* 66(4):692–703.
58. Rasmussen S, et al. (2015) Early divergent strains of Yersinia pestis in Eurasia 5,000 years ago. *Cell* 163(3):571–582.
59. Benedictow OJ (2012) *The Black Death 1346-1353: The Complete History* (Boydell Press, Suffolk, UK), 1st Ed.
60. Fyfe RM, Woodbridge J, Roberts N (2015) From forest to farmland: Pollen-inferred land cover change across Europe using the pseudobiomization approach. *Glob Change Biol* 21(3):1197–1212.
61. Woodbridge J, et al. (2014) The impact of the Neolithic agricultural transition in Britain: A comparison of pollen-based land-cover and archaeological 14C date-inferred population change. *J Archaeol Sci* 51:216–224.
62. Lechterbeck J, et al. (2014) Is Neolithic land use correlated with demography? An evaluation of pollen-derived land cover and radiocarbon-inferred demographic change from central Europe. *Holocene* 24(10):1297–1307.
63. Gronenborn D, Strien H-C, Dietrich S, Sirocko F (2014) 'Adaptive cycles' and climate fluctuations: A case study from Linear Pottery Culture in western Central Europe. *J Archaeol Sci* 51:73–83.
64. Haak W, et al. (2015) Massive migration from the steppe was a source for Indo-European languages in Europe. *Nature* 522(7555):207–211.
65. Manning K, Colledge S, Crema E, Shennan S, Timpson A (2016) The cultural evolution of Neolithic Europe. EUROEVOL dataset 1: Sites, phases and radiocarbon data. *J Open Archaeol Data* 5:e2.
66. Brown WA (2015) Through a filter, darkly: Population size estimation, systematic error, and random error in radiocarbon-supported demographic temporal frequency analysis. *J Archaeol Sci* 53:133–147.
67. Parnell A (2015) Bchron: Radiocarbon dating, age-depth modelling, relative sea-level rate estimation, and non-parametric phase modelling (R Foundation for Statistical Computing, Vienna), R package version 4.1.2. Available at https://CRAN.R-project.org/package=Bchron.
68. Reimer P (2013) IntCal13 and Marine13 radiocarbon age calibration curves 0-50,000 years cal BP. *Radiocarbon* 55(4):1869–1887.
69. Dakos V, et al. (2012) Methods for detecting early warnings of critical transitions in time series illustrated using simulated ecological data. *PLoS One* 7(7):e41010.
70. Best D, Gipps P (1974) Algorithm as 71: The upper tail probabilities of Kendall's tau. *Appl Stat* 23(1):98–100.
71. Torrence C, Compo GP (1998) A practical guide to wavelet analysis. *Bull Am Meteorol Soc* 79(1):61–78.
72. Gouhier T (2014) biwavelet: Conduct Univariate and Bivariate Wavelet Analyses, Version 0.17.4. Available at https://github.com/tgouhier/biwavelet.
73. R Core Team (2015) *R: A Language and Environment for Statistical Computing* (R Foundation for Statistical Computing, Vienna).